Forecasting Research

Forecasting Research Division
Scientific Paper No. 28

On the use of radiosonde humidity observations in mid-latitude NWP

by

A.C. Lorenc, D. Barker, R.S. Bell, B. Macpherson and A. J. Maycock

4th November 1994

Meteorological Office
London Road
Bracknell
Berkshire
RG12 2SZ
United Kingdom

Forecasting Research

Scientific Paper No.28

On the use of radiosonde humidity observations in mid-latitude NWP

by

A.C. Lorenc, D. Barker, R.S. Bell,
B. Macpherson and A.J. Maycock

4th November 1994

Forecasting Research
Meteorological Office
London Road
Bracknell
Berkshire RG12 2SZ
ENGLAND

Forecasting Research Scientific Paper 28
Submitted for publication in *Meteorology and Atmospheric Physics*.
printed 4 November 1994

Meteorological Office, Bracknell, England

On the use of radiosonde humidity observations in mid-latitude NWP

A. C. Lorenc, D. Barker, R. S. Bell, B. Macpherson, and **A. J. Maycock**

With 17 figures.

4th November 1994

Summary

We compare radiosonde observations of relative humidity with NWP versions of the Meteorological Office Unified Model, and attempt to understand the causes of the systematic differences seen. The differences are found to have a different structure in cyclonic and anticyclonic situations over the UK. In cyclonic situations the mid-tropospheric temperature and humidity differences could be due to model biases, consistent with the conservation of energy; the latent heating from precipitation of the model's excess moisture would remove the model's cold bias. There is also some evidence for observational bias. Wetting of the sonde sensor in cloud can cause a moist bias at higher levels. The Väisala RS80 sonde also appears to have a dry bias near saturation.

The Unified Model has a parametrisation for stratiform cloud which calculates the fractional cloud cover in a grid-box from the box-average relative humidity, allowing for sub-grid-scale variability within the box. This scheme has been tuned to give reasonable cloud amounts with the model's relative humidities. The cloud amounts implied (by the scheme) for radiosonde relative humidities are systematically less than the observed cloud. So assimilation of the observed humidities can significantly degrade analyses and predictions of cloud. Bias corrections for the radiosonde humidities have been calculated to compensate for this.

Experiments have been performed to test the effect of the bias correction on the assimilation and prediction of cloud and precipitation. With the control system, cloud cover and precipitation spins-up during the forecast period; the bias correction improves this. A large improvement was also found when the relationship between the temperature and humidity assimilation was changed; it is better to assume that temperature and relative humidity errors are uncorrelated, rather than temperature and specific humidity.

1. Introduction

In active mid-latitude weather systems, the distribution of humidity is largely determined by the vertical motions generated by the large scale dynamics. If a Numerical Weather Prediction (NWP) model assimilation system has an adequate representation of the flow pattern, and of the surface evaporation, it can generate a fairly realistic humidity pattern without using any humidity data (Lorenc and Tibaldi 1980). Accurate specification of initial humidities is more important in the forecasting of systems with weaker dynamical forcing, such as weak fronts, and layer cloud such as stratocumulus. It is also important if we are to get the correct cloud and precipitation in the assimilation and first few hours of the forecast, before the dynamically controlled advection has had time to generate its own humidity structures. This is the main motivation behind this work. A secondary motivation was to validate the NWP model humidities, eventually to guide tuning and development of model parametrisation schemes. The correct specification of humidity in convective situations is also very important, especially in the tropics, but it is not a major concern of this paper.

We consider the use of radiosonde humidity data to improve the humidity fields generated by the assimilation model. Radiosondes have high vertical resolution, capable of defining the base and thickness of cloud layers. They also give the only operationally available upper-air data with an absolute calibration; satellite data are calibrated against them, or against a model. It is therefore worthwhile paying attention to their correct use, despite the fact that satellite data give a much better horizontal coverage.

In section 2 we describe the UK Met Office Unified Model Assimilation system. The thresholds within the model for cloud and precipitation formation are critical in determining the model's humidity in the situations of most interest to forecasters. In section 3 we discuss the differences between the model's humidities, and radiosonde observations, concentrating on the UK. These data help us understand model biases (section 4), although there also seem to be some observational biases. In section 5 we consider the effect of assimilating humidities on model cloud. In our mesoscale system detailed cloud data are available from satellite, radar and surface observations. Radiosonde observations need to be bias corrected to be consistent with the model's cloud threshold if they are not to damage the cloud fields from direct assimilation of cloud observations. In section 6 we present experiments aimed at getting the correct precipitation amounts during the assimilation and short-period forecasts. Preservation of relative humidities when correcting for the model's cooling bias is shown to be as significant as using bias corrections for the radiosonde humidity data similar to those needed for correct cloud assimilation. Finally in section 7 we summarise conclusions, and make some suggestions for further work.

2. Assimilation System

The UK Met Office Unified Model (Cullen 1990) is a primitive equation grid-point model, used both for NWP and climate modelling. In this paper we are mainly concerned with the mesoscale, limited-area, and global NWP configurations, with horizontal grid-lengths of about 17, 40 and 90km respectively. However validation of the model's physical parametrisations using humidity observations will be of use to the climate model; conversely all the parametrisations used in the NWP configurations have been shown to give realistic simulations in the climate model. The model's advection and diffusion is formulated in terms of total specific humidity q_T (i.e. vapour plus cloud) and liquid-water potential temperature θ_L. Each time-step it diagnoses from these temperature, relative humidity (*rh*), cloud water, and cloud fraction, based on a model of the variation of relative humidity within a grid box (Smith 1990). This process determines the relationship between relative humidity and cloud fraction (plotted in figure 1). In principle the assumed distribution of relative humidity should vary with grid-box size, and with atmospheric characteristics such as the stratification. However in the current versions a single distribution is assumed, with coefficients varying only with level. These coefficients were chosen so as to get correct cloud cover in climate simulations; we did not attempt to vary them in this work.

The assimilation into this model uses the Analysis Correction (AC) scheme (Lorenc *et al.* 1991). Surface pressure, temperature, wind, and moisture observations are inserted into the model each time-step over a period of a few hours. At each step the differences between the observed values and the corresponding current model value are weighted and spread according to the assumed model error covariance structure. Before assimilation, radiosonde soundings are pre-processed to give values corresponding to each of the model layers (shown in figure 2). The algorithm used for this was found to be important, as discussed in section 4. In the mesoscale configuration, moisture observations are deduced in a pre-processing step from cloud observations, and inserted in the model, as described in section 4. Temperature and moisture observations are processed independently in the AC scheme. The precise method for separating moisture and temperature was found to be important, and is discussed further in section 5.

3. Systematic differences between radiosondes and model

In this section a study is made of the effect of synoptic weather conditions on the humidity and temperature biases over the UK in October 1993. The UK area was chosen for its relatively high concentration of radiosonde observations from one type of radiosonde (currently the Väisala RS80). The 'spin-up' of the rainfall and moisture field in the first few hours of a forecast after the observations have been assimilated is known to be particularly bad over the UK (Lorenc 1994). The month of October 1993 was chosen as it presented an opportunity to study the effects of synoptic weather type on mean temperature, humidity and associated biases. The first 15 days corresponded to generally cyclonic weather conditions, followed by a period of generally anticyclonic

weather from days 16 to 31 over the UK.

The data is taken from the observation processing database (OPD) of the operational global assimilation. The OPD contains all observations passed to the NWP suite together with relevant diagnostic information such as quality control (QC) flags and observation (***O***) minus model field differences, for both the forecast background (***B***) and the analysis (***A***). In this section, the background value is taken from a previous 6-hour global forecast run interpolated to the radiosonde's ascent time and position. The data is stored on model levels.

The observed data used has passed QC checks, which in the case of relative humidity includes only a background check, i.e. only if ***O-B*** exceeds a given error is the observation rejected from the assimilation process. This limit is currently in the region of 70% to 80%, so the QC of humidity measurements is not as stringent as for other variables. For each period during the month, the temperature and relative humidity observed and background data are time-meaned at each model level, giving mean vertical profiles of observed variables and their bias with respect to the model value.

In the lower troposphere there were over 1100 data for both temperature and humidity at each level for the month and area studied. The number of humidity data decreases to about 90% of the number of temperature data above global model level 9 (at a pressure about 400 hPa) due to both equipment breakdown and failure to pass the QC background check. Similar failures drastically reduce the numbers of both temperature and humidity in the stratosphere (at level 14, about 150 hPa).

The mean temperature of radiosonde observations in both cyclonic and anticyclonic periods is plotted in figure 3. There is an inversion during the anticyclonic period, so that levels 1-4 are warmer on average during the cyclonic period, and above this region the warmer conditions are found during the anticyclonic period. The temperature mean ***O-B*** difference for each period is shown in figure 4. A model cool (or measured warm) bias exists throughout the middle troposphere during the cyclonic period. During the second period the bias is not so clear-cut. In and above the upper troposphere a positive bias increases with model level during both periods. Inter-comparisons of the various radiosondes used around the world are held every few years. One conclusion to be drawn from such studies is that temperature measurements do not suffer significantly from any large bias at these pressures. It is therefore assumed in this paper that the temperature difference is due to a model cool bias of about 0.2K in the lower to middle troposphere in cyclonic conditions. In both periods there exists a model cool bias in the upper troposphere which increases to about 1K in the stratosphere.

The mean relative humidity is plotted against model level in figure 5. During the cyclonic period the lowest levels are on average 10% moister than in the anticyclonic period. This difference increases in the subsidence region above the inversion to a maximum of 40% in the middle troposphere and decreases again above this. The

humidity mean ***O-B*** difference is shown in figure 6 for each period. There exists a humidity bias near the surface which increases to nearly zero in both cases at level 4. This behaviour mirrors that of the temperature bias in figure 4.

As relative humidity is a function of temperature and specific humidity, there exists the possibility that a moist bias is due to a cool temperature bias at constant specific humidity. However calculations show this effect to be an order of magnitude smaller than the biases shown here; there is a clear bias in specific humidity too.

It is noteworthy that the peak of the negative humidity bias in each curve in figure 6 corresponds to the top of the region above which the mean relative humidity decreases rapidly. This indicates that the model's moist troposphere does not extend as high as observed. Above the tropopause, the bias changes sign; the observations are moister. The accuracy of radiosonde humidity measurements is seriously reduced at levels above 200 hPa, so no comment is made on the origin of the high level bias.

The negative tropospheric humidity mean ***O-B*** difference could be due to a moist model bias or a dry bias in the radiosonde observations. The first possibility is discussed below. Possible humidity biases originating from the actual measurement are discussed in Section 5.

4. Possible causes of model biases

Here we investigate the hypothesis that the model's moist bias and its cool bias are both due to insufficient precipitation. The thermal energy E of an air parcel is the sum of its sensible and latent heats:

$$E = c_p T + Lq = c_p T + L q_s \frac{rh}{100} \qquad (1)$$

where c_p is the specific heat at constant pressure and L is the latent heat of vaporisation. Hypothesising that there are no significant errors in external sources of energy, and neglecting the dependence of the saturation specific humidity (q_s) on temperature, we can calculate the relative humidity bias which should correspond to a temperature bias:

$$\Delta rh \simeq \frac{100\ c_p}{q_s\ L}\ \Delta T \qquad (2)$$

This is plotted in figures 7 and 8 for the cyclonic and anticyclonic periods of October 1993, along with the actual humidity bias. It can be seen that the middle troposphere biases in the cyclonic period match the hypothesis rather well. Above level 8, the large ΔT shown in figure 4 cause the correction calculated in (2) to go off-scale, so it is not

plotted. At the tropopause the bias patterns in both temperature and humidity during the cyclonic period are consistent with the model's tropopause being too low. Since the balance between latent heating and radiative cooling helps determine the height of the tropopause, this also may be an indirect effect of insufficient precipitation.

In the boundary layer, and during the anticyclonic periods, not surprisingly it seems that effects other than precipitation are important. In the boundary layer insufficient precipitation may be a factor, but only accounts for about half the bias. In the stratosphere the observations are moister than the model, but this may be due to observational bias as discussed below.

5. Biases in radiosonde humidity observations

We first investigate further the stratospheric humidities. In clouds the radiosonde humidity detectors can be wetted. The radiosonde ascends to cooler levels which cause the detector to freeze. An erroneously large value of relative humidity can then be reported. The effect of this process can be seen in the large scatter of points near the top of figure 9, which shows a scatter plot of the relative humidity at the tropopause, against the highest value reached during the ascent, for UK soundings during October 1993. This wetting effect is not confined to the Väisala radiosondes used in the UK; the Canadian soundings (from VIZ sondes) for the same period give a similar plot (not shown).

A noteworthy feature of figure 9 is that the points apparently affected by wetting have not all reported saturation lower in the ascent; some are below saturation by up to 6%. (The Canadian VIZ soundings show more saturated ascents). This is consistent with comments from observers that sondes which have been seen to pass through cloud do not always show saturation in the reported sounding. Further evidence for a dry bias comes from radiosonde intercomparisons, which frequently indicate low values of relative humidity from Väisala sondes compared to others and suggest a dry bias in cloud of 3-5% (Nash, personal communication), and from intercomparison between a sonde and the Met Research Flight aircraft (McKenna, personal communication). Väisala radiosondes are not currently calibrated in the range 80% to 100%, which may lead to bias in the range of humidities of most interest to meteorologists. Wade and Schwartz (1993) have reported similar problems with a different make of sondes.

The clearest examples of the damage caused by the systematic differences between the radiosonde humidities in or near clouds and the model, occur in the mesoscale configuration. A Moisture Observation Preprocessing System known as MOPS, (Wright *et al*, 1994) is used to prepare a three-dimensional cloud cover analysis from satellite images, radar rain, and surface observations. This is converted to an equivalent relative humidity using the relationship plotted in figure 1. The model is nudged towards these humidities each step, as part of the AC scheme. Since they are available at every grid-point, no horizontal spreading is done. It has been found that this process improves the model's representation of stratocumulus cloud during the assimilation and short-period

forecast. Benefit from this cloud data can last up to 18 hours into the forecast in anticyclonic conditions (Wright *et al*, 1994). However when radiosonde humidities are also assimilated, their lower values sometimes cause large gaps in the cloud cover around each station (figure 10).

One contribution to this effect was found to be the pre-processing of radiosonde observations to model layers. In the original system this was done by averaging the observed temperature and relative humidity profile for each model layer. In stratified situations, this gave an average relative humidity significantly less than the maximum in the layer. Because the model does not allow for increased variability of sub-grid-scale relative humidity in such situations, the lower relative humidity significantly reduces the implied cloud amount. For radiosondes pre-processed to the 31 layers of the mesoscale model, the mean cloud error was 1.90 oktas in a sample month for UK soundings (table 1, row 1). For soundings averaged to the 19 thicker layers of the limited-area model the bias was 2.85 oktas. Methods for making the model's parametrisation allow for stratification and layer thickness are being investigated, but in the interim it was found better to use point values of humidity. Both the layer maximum, and the value interpolated to the layer mid-point were tested, both by looking at individual soundings, and for their effect on the overall bias (table 1). The layer maximum method was rejected because it led to inferior vertical structure in which dryer layers were poorly represented.

MODEL	Method	Mean Error	RMS Error
Mesoscale	layer average	-1.90	3.09
Mesoscale	layer maximum	-0.29	2.70
Mesoscale	interpolation to layer mid-point	-1.39	2.83
Mesoscale	interpolation + bias correction	-0.68	2.51
Limited Area	layer average	-2.85	3.85
Limited Area	layer maximum	-0.41	2.77
Limited Area	interpolation to layer mid-point	-2.04	3.43
Limited Area	interpolation + bias correction	-0.88	2.82

Table 1: Errors in implied cloud cover from radiosondes relative to surface cloud reports, for different profile pre-processing options. Data for April 1994.

Even after this change, there is still an appreciable bias between the cloud cover from surface observations at radiosonde stations and the cloud deduced from the radiosonde humidity soundings via the model's relative humidity - cloud relationship and the

assumption of maximum-random cloud layer overlap. The distribution of this bias with cloud amount is shown in figure 11. From these data it is possible to work out a bias correction to the radiosonde humidities, to reduce the bias in implied cloud. This is shown in figure 12 as a function of the observed relative humidity. The bias correction is

$$\Delta rh = rh(C_{obs}) - rh(C_{sonde}) \tag{3}$$

where the surface observation C_{obs} takes values in oktas from 1 to 8 and C_{sonde} is the average implied cloud cover from radiosondes collocated with the surface reports for a specified value of C_{obs}. The function $rh(C)$ is that plotted in figure 1. Treating Δrh as a function of the average relative humidity $rh(C_{sonde})$, the data in figure 12 are approximately fitted by the piece-wise linear function shown:

$$\Delta rh = \begin{cases} 0 & for\ rh_{ob} < rh_{crit} \\ \dfrac{rh_{ob} - rh_{crit}}{92 - rh_{crit}} \times 3.0 & for\ rh_{crit} < rh_{ob} < 92 \\ 3.0 & for\ 92 < rh_{ob} < 96.5 \\ \dfrac{100 - rh_{ob}}{100 - 96.5} \times 3.0 & for\ 96.5 < rh_{ob} < 100 \\ o & for\ rh_{ob} = 100 \end{cases} \tag{4}$$

The value of rh_{crit} is set at 80%, since this is the upper limit for calibration of Väisala sondes, and is about the value where the model starts forming clouds. For the limited area version, the data are best described by a maximum correction of 4.6% between 90% and 95%.

When this bias correction is added to the effect of using interpolated rather than averaged values, the mean and RMS errors in implied cloud are further reduced (table 1). The maximum bias corrections of 3% for the mesoscale and 4.6% for the limited area version are consistent with the magnitude of the dry bias of Väisala sondes in cloud quoted above. This statistically derived correction can be seen mainly as an attempt to correct for the mean dry observational bias in cloud, but in a manner consistent with the model cloud scheme and the residual effects of vertical resolution which remain after interpolation to layer mid-points. A true observational bias would be independent of model vertical resolution and would logically be applied before pre-processing of the observed profiles onto model layers.

How much more reduction in implied cloud errors from sondes should be sought ? Of course it is true that even with a perfect humidity sensor and an 'exact' model cloud

scheme, one would not obtain perfect agreement between cloud diagnosed from a radiosonde and a surface observation at the launch site. The sonde will sample along a particular wind-dependent trajectory. In situations of only partial cloud cover, this will give different cloud amounts from surface observations which represent an average over an area that expands with height. Thus random differences are inevitable although, over a period of time, differences in partial cloud sampling should not lead to a bias relative to surface observations. In other words, a large number of radiosondes released simultaneously ought to return a mean implied cloud cover closer to the surface report than a single ascent.

One reason for permitting some discrepancy between radiosondes and cloud observations, at least for low partial cover, lies in the split between the model's parametrisations of stratiform and convective cloud cover. The relationship between relative humidity and cloud fraction applies only to stratiform cloud. Convective cloud is diagnosed separately in the model, though amounts are small in the mean and reach a local maximum of only around 3 oktas in the mesoscale version. It would be unwise to correct completely for a bias between sonde cloud observations and surface reports of partial cover, since the latter may reflect a real convective contribution which we should not attempt to reproduce in the grid-scale humidity field of the model.

A reasonable target for agreement between different sources of cloud data to be assimilated would be an rms difference equal to the error of representativeness of a surface cloud cover report at the model grid-scale. A study of cloud cover differences between neighbouring stations (Golding, personal communication) has shown this to be around 1.5 oktas for separations of about 17km (the mesoscale configuration grid-length), rising to about 2 oktas for 50km. 1.5 oktas is still significantly below the rms error remaining after mid-point interpolation and the present bias correction. Some of this difference is due to errors in the radiosonde observations and processing, and some to inadequacy of the model's humidity cloud relationship. But there is probably still scope for further improvement. One avenue to explore would be a real-time bias correction to replace the current statistical one. Each ascent would be 'calibrated' against its surface observation. This approach would have the advantage of modifying the corrections applied if either the model cloud scheme or the quality of the radiosonde changed. The present statistical correction parameters need to be reviewed periodically.

6. Correction of rainfall and cloud spin-up

A weakness of the current limited-area model (LAM) forecasts is the lack of precipitation and cloud in the early stages (0-12 hours), relative to the later forecast periods. This adjustment during the early stages of a forecast is often called a 'spin-up'. It has been a characteristic of most data assimilation systems for many years and is usually attributed to suppressed dynamical activity due to the initialisation process. We have no reason to suspect such a problem in the Met. Office system (section 2) since there is no explicit initialisation step. However, some feature of the assimilation process, or the

observational data which are assimilated, is responsible for a moisture deficiency which causes this spin-up. The same problem appears in the global model, where it is less important since that forecast period is of less value, but it is a possible contributor to another problem. When the soil moisture is allowed to evolve freely during an extended global data assimilation cycle, there is a marked drying out of the model soil surface. This is unacceptable since it impacts adversely on convection and surface temperature forecasts over land, thus at present within the operational system, the soil moisture field is reset regularly to climatological values.

The LAM system takes the initial conditions for its assimilation (12 hours before nominal analysis time) and boundary conditions, from the global system. Because of this it is unsuitable for testing the full effect to changes in the humidity assimilation, which often take several days to have their full effect. We therefore performed a series of experiments (listed in table 2) with the global system. The basic experiment consisted of a 3 day global data assimilation followed by a 2 day forecast. Diagnostic information from the control experiment (a) confirmed that the case chosen exhibits the sort of problems noted in the monthly mean verification data. We display this diagnostic information in figure 13 in the form of time-series of globally averaged precipitation and high, medium, low cloud respectively. Note the 12 hour periodicity during the assimilation cycle with reductions coinciding with the introduction of radiosonde humidity data in the period running up to the main synoptic hours. Note also the mean level of both precipitation and total cloud during the assimilation cycle (1-432 time-steps) is significantly less than in the forecast. For precipitation, the assimilation value is 0.26×10^{-4} increasing to a forecast value of 0.32×10^{-4} (in SI units of kg m^{-1} s^{-1}; which in mm/day is 2.2 increasing to 2.8); the latter value being more in accord with climatological expectation. For total cloud cover, the assimilation value is 43% increasing to a forecast value of 51%. Even the latter value is on the low side compared with climatological estimates of near 60% (e.g. from ISCCP, Rossow *et al.*, 1993).

Experiment	3 day assimilation and 2 day forecast with global system:
(a)	Control. Operational system as in September 1994.
(b)	No humidity observations used.
(c)	Radiosonde humidity observations bias corrected for humidities $>80\%$.
(d)	rh assumed to be independent of T (rather than q independent of T).
(e)	c & d. rh independent of T, & humidity observations bias corrected.

Table 2. Experiments performed with the global assimilation & forecast system.

6.1 (b) No humidity observations

After the control, experiment (b) was run without any humidity observations. The precipitation and total cloud cover time-series for this run (superimposed on the control) is given in figure 14. We see the periodicity has been much reduced and the level of the precipitation during the assimilation has been increased to about 0.29×10^{-4}, which is still significantly down on the forecast value. Given the 'improvement' in the statistics, we might be tempted to say that since the humidity field is largely governed by the model dynamics, we can let it evolve without using humidity observations. Figures 15 and 16 illustrate the 700hPa relative humidity fields at the end of the assimilation period (T+0), and after 24hours forecast (T+24), obtained from the control and experiment (b) without humidity observations. The validation of these runs (fit to radiosonde rh observations) is given in table 3.

Verification Area	**Experiment**	**T+0**	**T+24**
Northern Hem (90-30N)	(a) Control	9.0	20.5
" "	(b) No rh obs	19.4	21.3
Tropics (30N-30S)	(a) Control	8.7	18.4
" "	(b) No rh obs	21.3	21.7

Table 3. RMS fit to radiosonde rh observations (%), of runs with and without humidity observations.

We see substantial differences in the relative humidity fields from these two experiments, particularly at T+0, but even at T+24. The validation shows a substantial impact at T+0, but only a marginal impact at T+24 (more so in the tropics where dynamic forcing is weaker). This suggests that at least in this 0-24 hour timescale the humidity observations are likely to be important (although with a degree of importance diminishing with time), more so if the bias problem can be addressed.

6.2 Boosting radiosonde rh

Experiment (c) made use of humidity observations but incorporated a scaling to boost the observation values near saturation. For this experiment with the global model a quadratic correction was tried. Values of the original layer mean observation (rh_{ob}) between 80% (rh_{crit}) and 100% were boosted by:

$$\Delta\, rh = \alpha\,(100-rh_{ob})(rh_{ob}-rh_{crit}) \quad for\ rh_{ob}>rh_{crit} \qquad (5)$$

where α should not exceed $(100-rh_{crit})^{-1}$ and was in fact set to that maximum value.

We see in figure 14 that experiments (b) and (c) are rather similar for precipitation (both about 0.29×10^{-4} during the assimilation period), indicating that the observations can be assimilated without the adverse impact with an appropriate boost near saturation. There is less impact on the cloud diagnostics in this experiment than the first.

6.3 Conserving rh during temperature assimilation

Whether we ignore radiosonde humidity reports, or attempt to compensate for possible bias, we are still left with a deficiency in rainfall during the assimilation cycle. The next experiment identified the contribution to this deficiency due to temperature reports. We note that the model has a cold bias. In the control assimilation, the temperature observations reduce the relative humidity as they warm the model, because the model's mixing ratio is preserved during the temperature assimilation. We have addressed the problem in experiment (d) by instead preserving relative humidity during the temperature assimilation. Note the increased level of precipitation shown in figure 14. The results from this experiment differ from (a) (b) and (c) in respect of cloud, where a substantial increase is evident. This large impact is because the temperature increments cover a wider area and have larger weights than the humidity increments, so (a) and (d) differ in their changes to humidity at more points, even where the humidity was previously far from saturated. The periodicity is still present since we have done nothing in this run to change the assimilation of radiosonde humidity observations.

6.4 The combined option

Experiment (e) includes both the changes tested in experiments (c) and (d). We see in figure 14 that after an initial adjustment during the first 24 hours of the assimilation, the average values settle down to a level which is comparable to that obtained in the first couple of days of the forecast. To study this further, look at figure 17, which shows the high, medium and low cloud fractions for experiment (e), with the forecast period extended to four days. Although the spin-up during day 1 of the forecast has been removed (time-step 432-576), there still seems to be an upward trend to the high and to a lesser extent medium cloud later in the forecast which might be a pointer to a model bias problem. A by-product of the increased precipitation during the assimilation is a lessening of the land surface drying in the model, from 0.5% per day to 0.1% per day in the global average.

A similar system has been put though an extended parallel trial versus the operational (control) system. Much improved cloud and rainfall forecasts were obtained for the UK area in the first 12 hours of the forecasts. The increased precipitation reduced the model's tropospheric cooling bias by about one third in the 24hour forecasts, significantly improving verification scores for geopotential. Evolution of the soil moisture content during the assimilation was more realistic. Implementation of the changed system is planned later in 1994.

7. Conclusions

We have shown that with careful scrutiny of the fit to radiosonde observations in an assimilation scheme, we can gain useful insights into the weaknesses of the model. In particular part of the cooling and moistening biases in the model's mid-latitude troposphere seem both to be related (in cyclonic situations) to a lack of precipitation. The model's parametrisation of stratiform cloud, based on an assumed distribution of relative humidity within a grid-box, does not adequately represent thin cloud layers in stratified situations.

The possibility of observational bias makes it difficult to identify all differences with model biases. In particular we have presented evidence for moist observational bias at and above the tropopause, caused by wetting in cloud. For Väisala sondes at least there seems to be a dry observational bias in the troposphere at high humidities. These difficulties highlight the importance of efforts to get more accurate humidity observations.

In designing the best assimilation scheme for radiosonde humidities, both types of bias must be considered. Because the UM has a tendency to cool, the assimilation of temperature observations causes positive temperature increments; care must be taken that these do not reduced the model's relative humidity. An equivalent statement is that, in the most important (moist) situations, temperature forecast errors are uncorrelated with relative humidity errors, rather than with specific humidity errors. Since accurate cloud and rain amounts are essential in the forecasting system, it is important to correct the humidities observed by radiosondes to be consistent with the assumptions in the model's parametrisation scheme. This is probably correcting an observational bias, although there may also be a bias implicit in the parametrisations. Implementation of these changes causes a significant improvement in short period forecasts.

This work has indicated that the following areas of future development may be profitable:

- Improved model parametrisation of thin layer clouds (or an increase in vertical resolution).
- Bias correction of individual radiosonde humidities, using the model's cloud scheme, to match the surface observations of cloud from SYNOP reports that are often available near radiosonde stations.
- Extension of the studies to other (mainly satellite) sources of humidity data. Initially these should be used to diagnose the model's and observations' weaknesses, which need to be understood before attempting to assimilate the data.

References

Cullen, M. J. P., 1990
"Introduction to the unified forecast/climate model". UMDP1, Forecasting Research Div., UK Met Office.

Lorenc, A. C., 1994
"Assimilation of Satellite Data in Models for Energy and Water Cycle Research". *Adv. Space Res.*, **14**, (1)145-(1)154.

Lorenc, A. C. and S. Tibaldi, 1980
"The treatment of humidity in ECMWF"s data assimilation scheme". *Atmospheric Water Vapour* ed. A. Deepak, T. Wilkinson and L. H. Rubnke, 497-512. Academic Press, New York.

Lorenc A. C., R. S. Bell and B. Macpherson, 1991
"The Meteorological Office Analysis Correction Data Assimilation scheme", *Quart J R Met Soc*, **117**, 59-89

Maycock A. J, and B. Macpherson, 1994
"Developments in mesoscale data assimilation at the UK Met Office", *proc 10th AMS conf on NWP*, Portland, 561-563

Rossow W. B., A. W. Walker and L. C. Gardner, 1993
"Comparison of ISCCP and Other Cloud Amounts", *Journal of Climate*, **6**, 2394-2418

Smith, R.N.B., 1990
"A scheme for predicting cloud layers and their water content in a general circulation model". *Quart.J.Roy.Met.Soc.*, **116**, 435-460

Wade C. G. and B. Schwartz, 1993
"Radiosonde humidity observations near saturation", *proc 8th AMS conf on Met Obs, Anaheim*, 44-49

Wright B.J., W.H.Hand and B Macpherson, 1994
"Assimilation of satellite data for mesoscale analysis", *proc 1993 ECMWF Seminar on 'Developments in the Use of Satellite Data in Numerical Weather Prediction'*, 111-128

LEGENDS FOR FIGURES

Figure 1 Relationship between grid-box mean relative humidity and cloud fraction in the model cloud scheme. The critical threshold for cloud formation is 85% in this case.

Figure 2 Layer boundaries (full lines) and levels (dashed lines) for the 19 levels used in climate global NWP and regional NWP, and the 31 levels used in mesoscale NWP.

Figure 3 Model level mean temperature for UK radiosondes during cyclonic (1st to 15th) and anticyclonic (16th to 31st) periods in October 1993.

Figure 4 Model level ***O-B*** temperature bias for UK radiosondes during cyclonic (1st to 15th) and anticyclonic (16th to 31st) periods in October 1993.

Figure 5 Model level mean relative humidity for UK radiosondes during cyclonic (1st to 15th) and anticyclonic (16th to 31st) periods in October 1993.

Figure 6 Model level ***O-B*** relative humidity bias for UK radiosondes during cyclonic (1st to 15th) and anticyclonic (16th to 31st) periods in October 1993.

Figure 7 Actual ***O-B*** relative humidity bias for UK radiosondes during the cyclonic period, and that from (2) consistent with the temperature bias (in figure 4) and energy conservation.

Figure 8 Actual ***O-B*** relative humidity bias for UK radiosondes during the anticyclonic period, and that from (2) consistent with the temperature bias (in figure 4) and energy conservation.

Figure 9 The maximum relative humidity measured by each UK radiosonde sounding during October 1993, plotted against the relative humidity measured at the tropopause.

Figure 10 Example of the impact of radiosonde humidity data in removing cloud from mesoscale model analyses. Both frames show t+0 total cloud cover, with areas of less than 3 oktas cover shown clear. The left-hand frame is the operational analysis, the right-hand frame is from an analysis omitting radiosonde humidity data. At analysis time, 0 UTC 2nd November 1993, all UK stations were reporting full cover of stratocumulus.

Figure 11 Implied cloud cover from radiosondes as a function of observed cloud cover at collocated surface stations. The radiosonde data are from UK stations for the period April-June 1994 and have been pre-processed onto

mesoscale model layers by interpolation to the layer mid-points.

Figure 12 Relative humidity bias correction as a function of observed radiosonde relative humidity (after interpolation to layer mid-points). The plotted points were derived from equation (3) and the data for mesoscale resolution in figure 11. The piece-wise linear fit to the data shown is given by equation (4).

Figure 13 Time-series of global average precipitation rate (in 10^{-4} kg m^{-1} s^{-1}) and low medium and high fractional cloud cover, from the control experiment. This consisted of 3 days' assimilation (144 time-steps=1 day) followed by a 2 day forecast, for a case in October 1993.

Figure 14 Time-series of global average precipitation rate (in 10^{-4} kg m^{-1} s^{-1}) and total fractional cloud cover, from the experiments listed in table 2, for a case in October 93. The plots each show one of experiments (b) (c) (d) or (e), with the control experiment (a) shown dotted.

Figure 15 700hPa relative humidity field after 3 days' assimilation, for experiments (a) control, and (b) without humidity observations.

Figure 16 700hPa relative humidity field after 3 days' assimilation and 1 day forecast, for experiments (a) control, and (b) without rh observations.

Figure 17 Time-series of low medium and high fractional cloud cover, from experiment (e). This consisted of 3 days' assimilation (144 time-steps=1 day) followed by a 4 day forecast. The control experiment (a), is shown dotted for comparison.

corresponding author's address:
Andrew C Lorenc
Forecasting Research
Meteorological Office
London Road, Bracknell, Berkshire, RG12 2SZ
United Kingdom
Telex: 849801
International fax: +44 1344 854026
International tel: +44 1344 856227
E-mail: aclorenc@email.meto.gov.uk

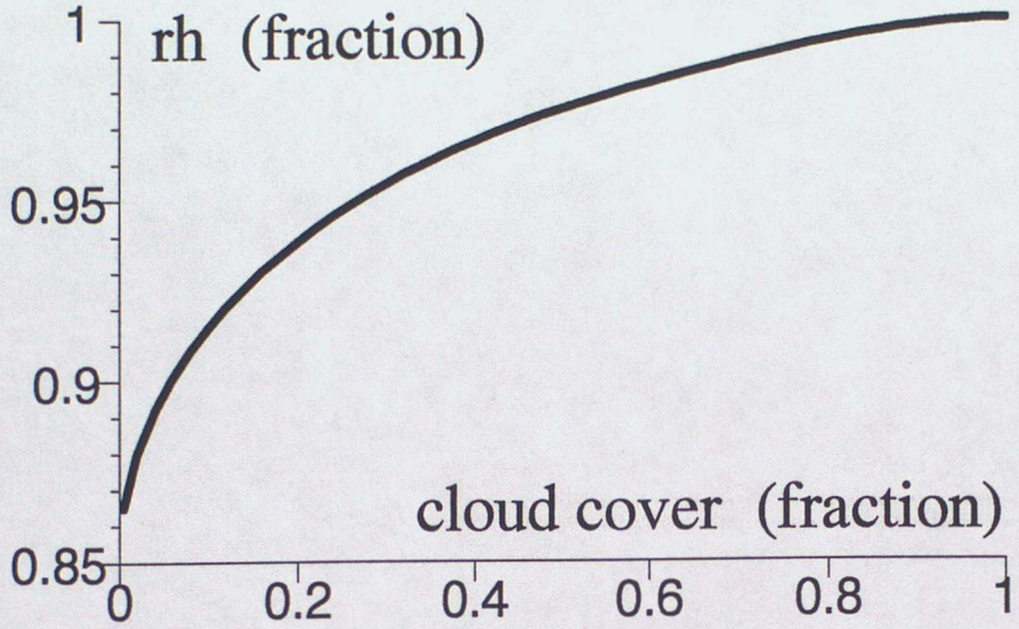

Figure 1 Relationship between grid-box mean relative humidity and cloud fraction in the model cloud scheme. The critical threshold for cloud formation is 85% in this case.

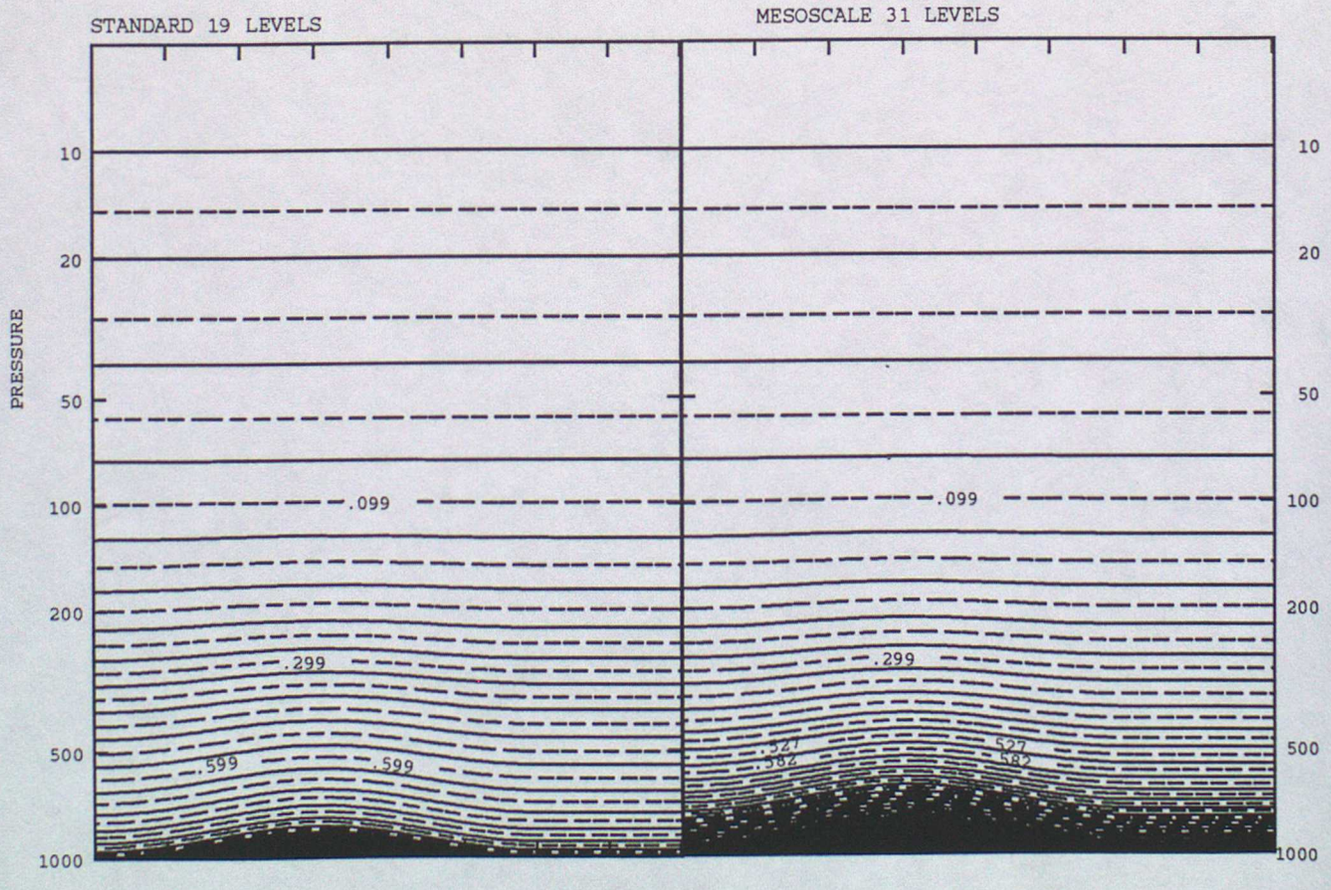

Figure 2 Layer boundaries (full lines) and levels (dashed lines) for the 19 levels used in climate global NWP and regional NWP, and the 31 levels used in mesoscale NWP.

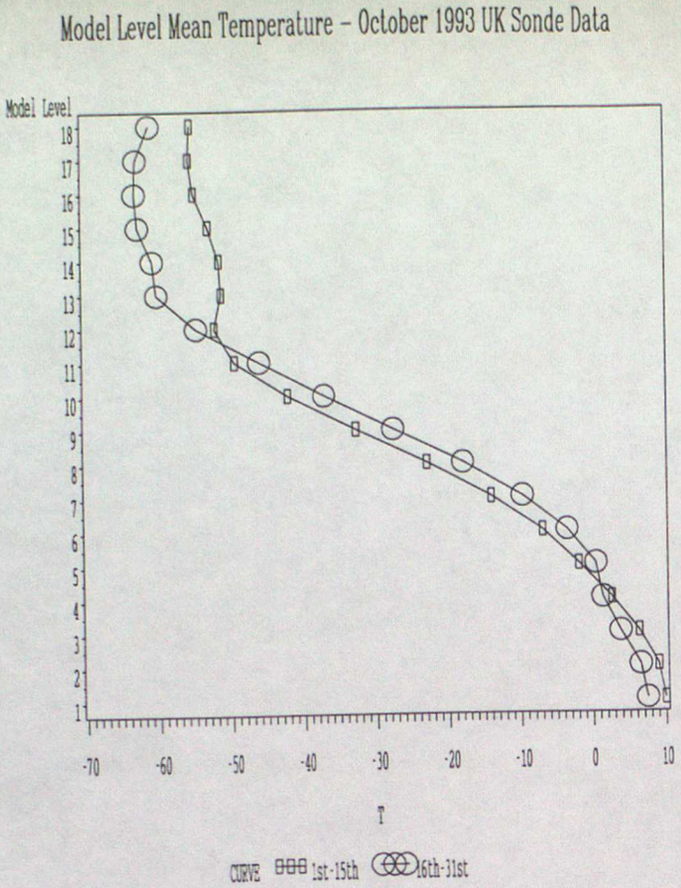

Figure 3 Model level mean temperature for UK radiosondes during cyclonic (1st to 15th) and anticyclonic (16th to 31st) periods in October 1993.

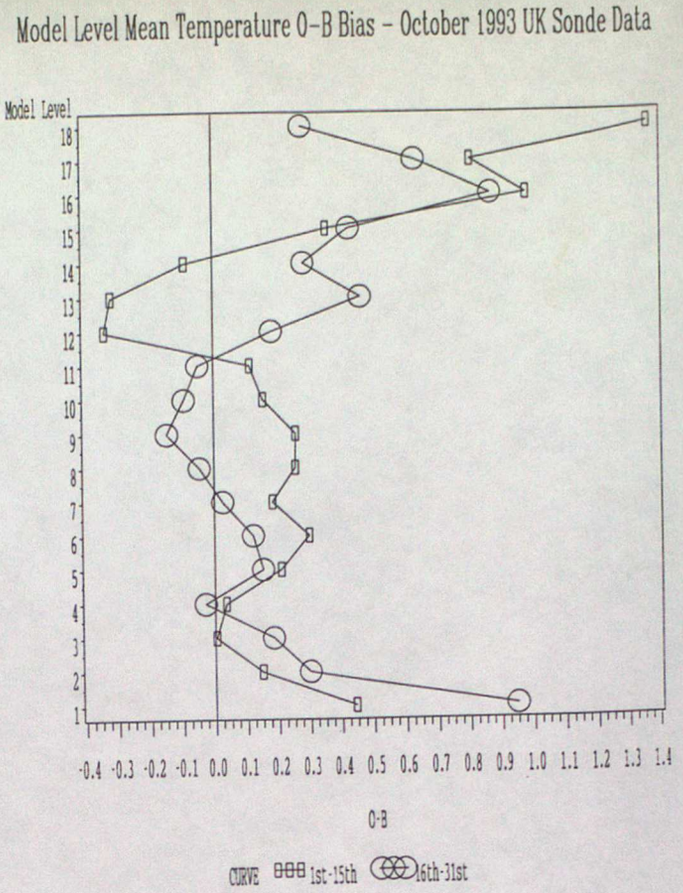

Figure 4 Model level ***O-B*** temperature bias for UK radiosondes during cyclonic (1st to 15th) and anticyclonic (16th to 31st) periods in October 1993.

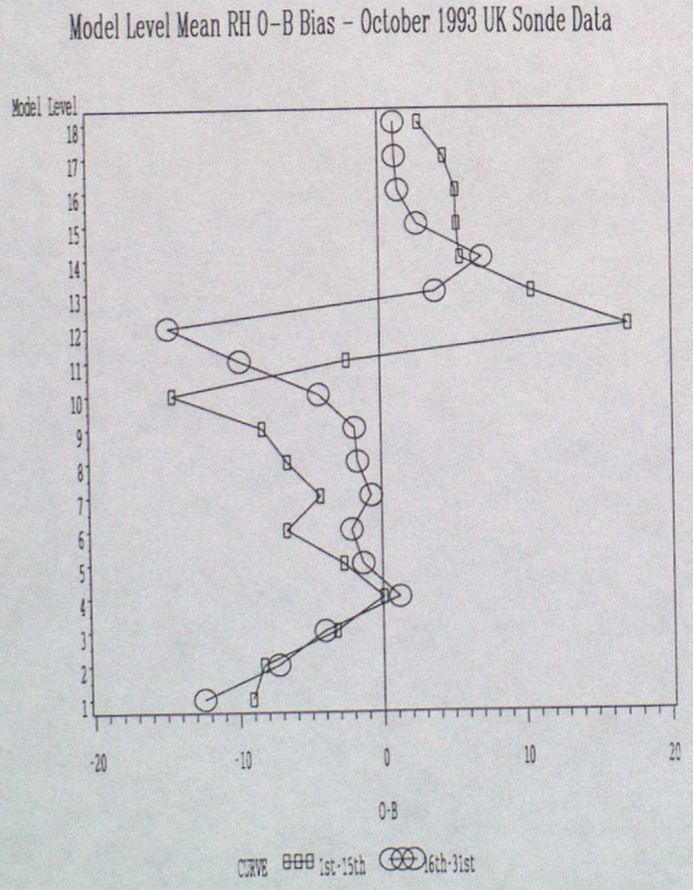

Figure 5 Model level mean relative humidity for UK radiosondes during cyclonic (1st to 15th) and anticyclonic (16th to 31st) periods in October 1993.

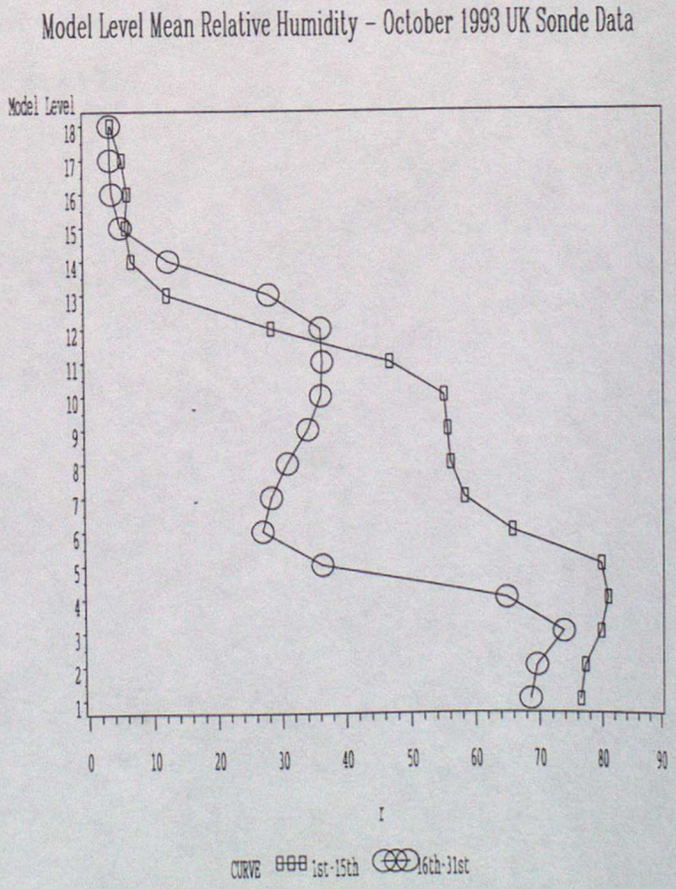

Figure 6 Model level ***O-B*** relative humidity bias for UK radiosondes during cyclonic (1st to 15th) and anticyclonic (16th to 31st) periods in October 1993.

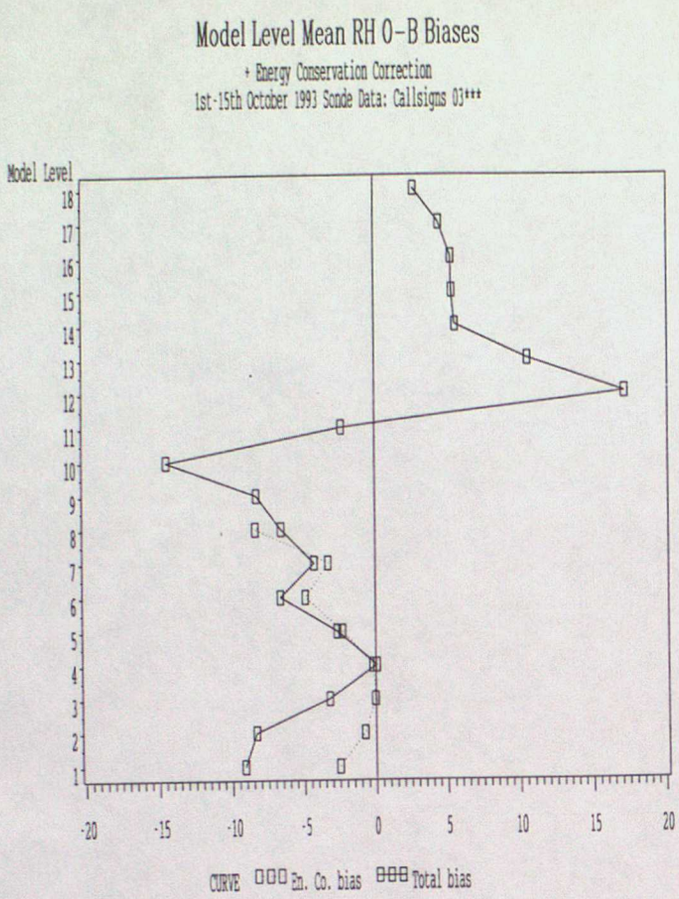

Figure 7 Actual ***O-B*** relative humidity bias for UK radiosondes during the cyclonic period, and that from (2) consistent with the temperature bias (in figure 4) and energy conservation.

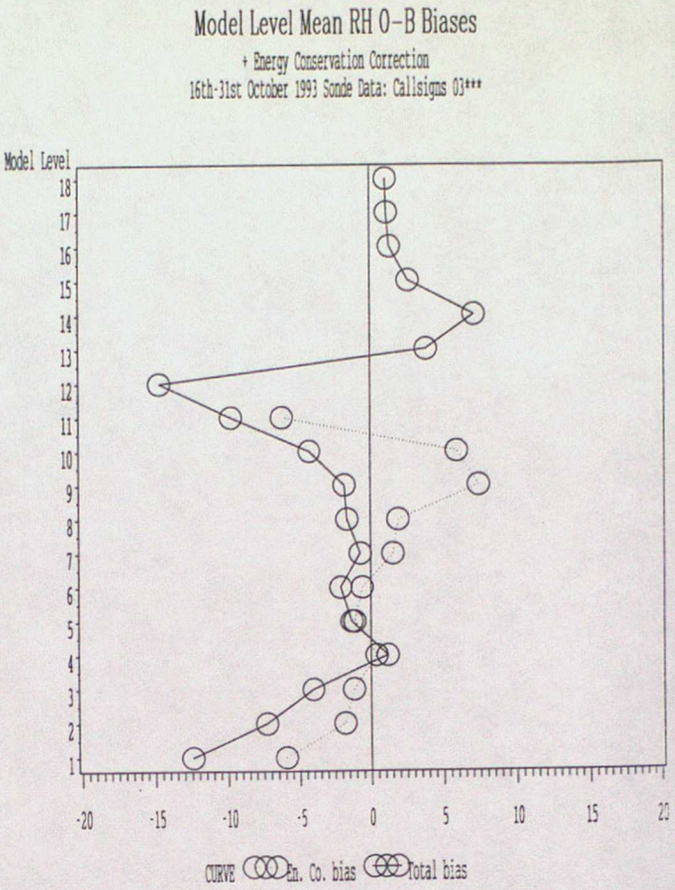

Figure 8 Actual ***O-B*** relative humidity bias for UK radiosondes during the anticyclonic period, and that from (2) consistent with the temperature bias (in figure 4) and energy conservation.

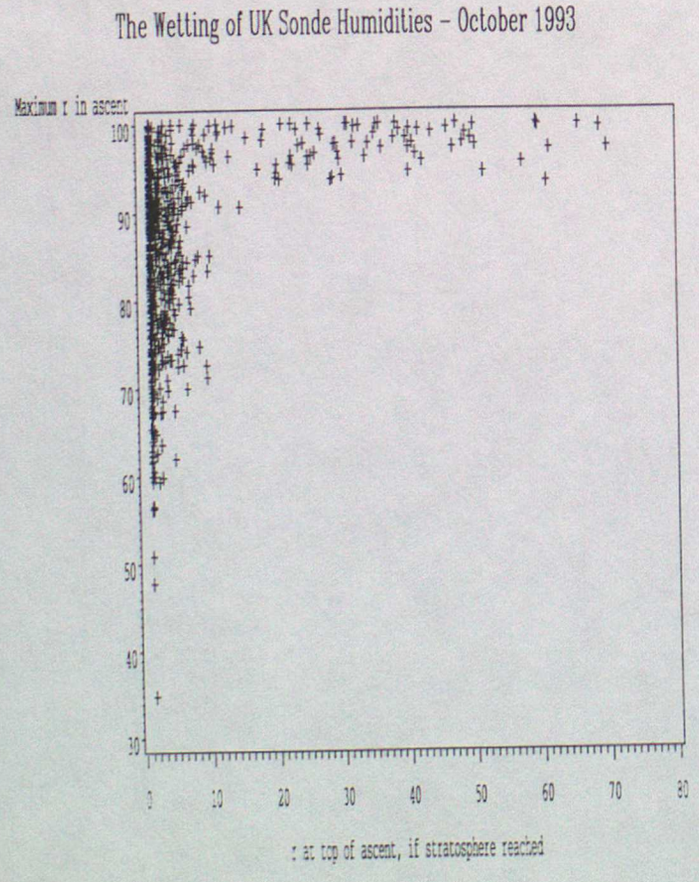

Figure 9 The maximum relative humidity measured by each UK radiosonde sounding during October 1993, plotted against the relative humidity measured at the tropopause.

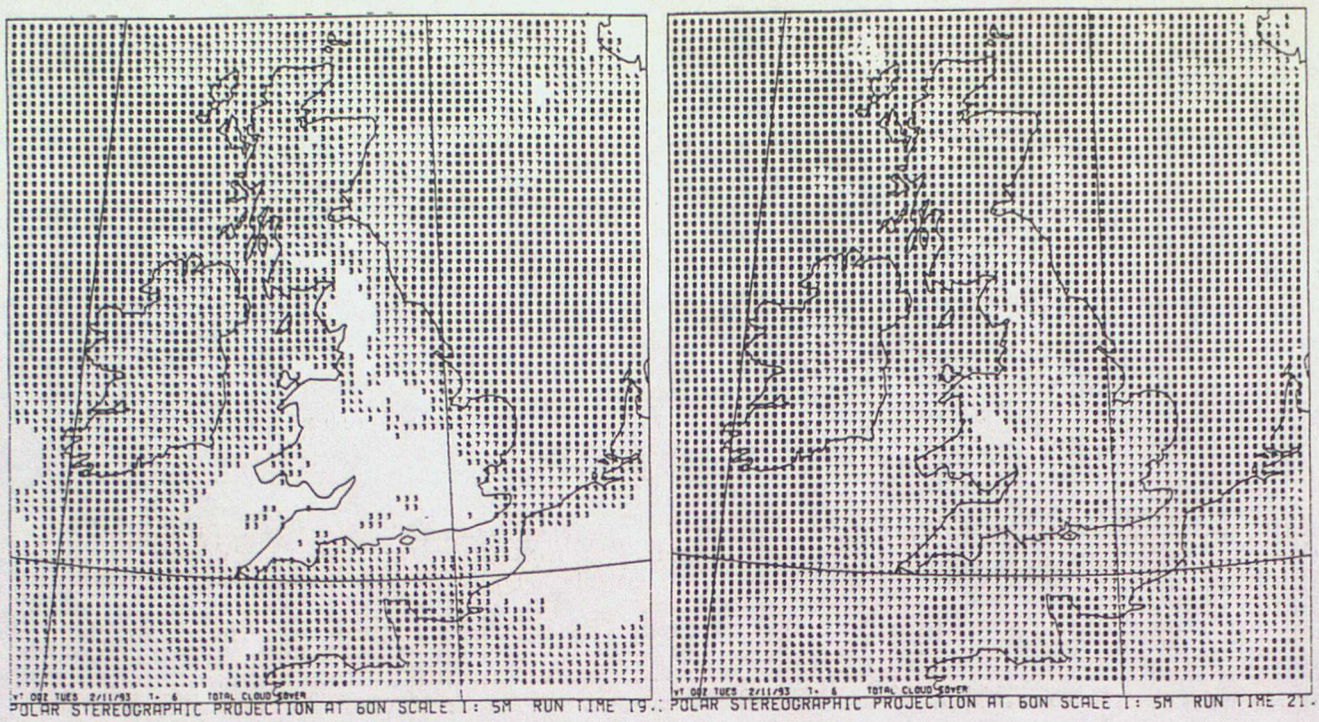

Figure 10 Example of the impact of radiosonde humidity data in removing cloud from mesoscale model analyses. Both frames show t+0 total cloud cover, with areas of less than 3 oktas cover shown clear. The left-hand frame is the operational analysis, the right-hand frame is from an analysis omitting radiosonde humidity data. At analysis time, 0 UTC 2nd November 1993, all UK stations were reporting full cover of stratocumulus.

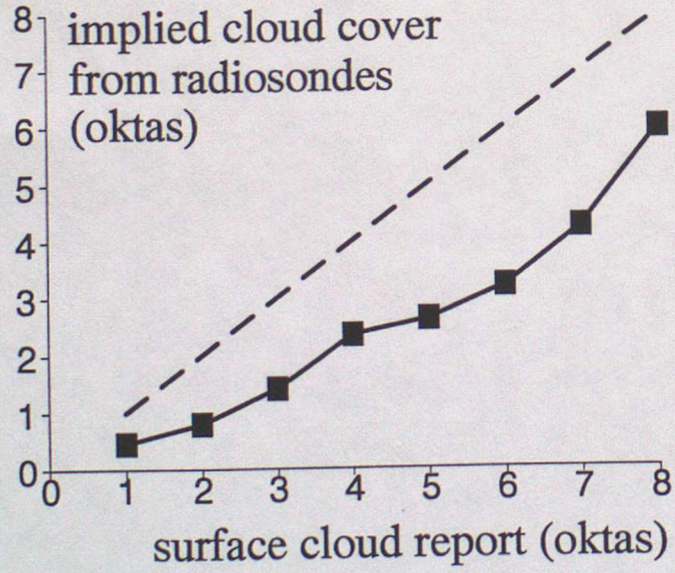

Figure 11 Implied cloud cover from radiosondes as a function of observed cloud cover at collocated surface stations. The radiosonde data are from UK stations for the period April-June 1994 and have been pre-processed onto mesoscale model layers by interpolation to the layer mid-points.

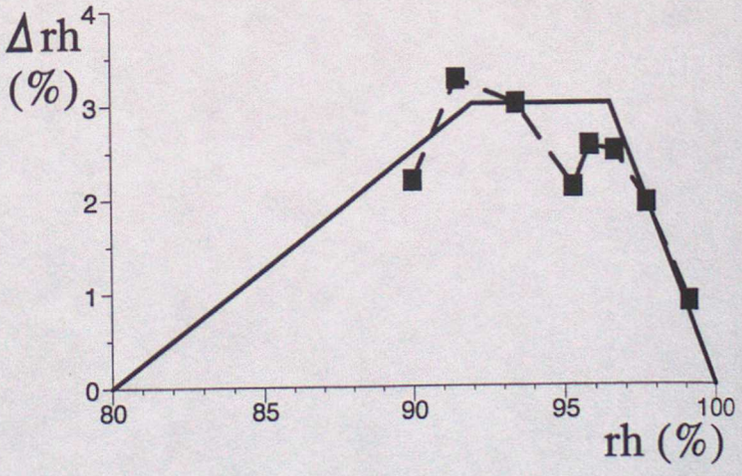

Figure 12 Relative humidity bias correction as a function of observed radiosonde relative humidity (after interpolation to layer mid-points). The plotted points were derived from equation (3) and the data for mesoscale resolution in figure 11. The piece-wise linear fit to the data shown is given by equation (4).

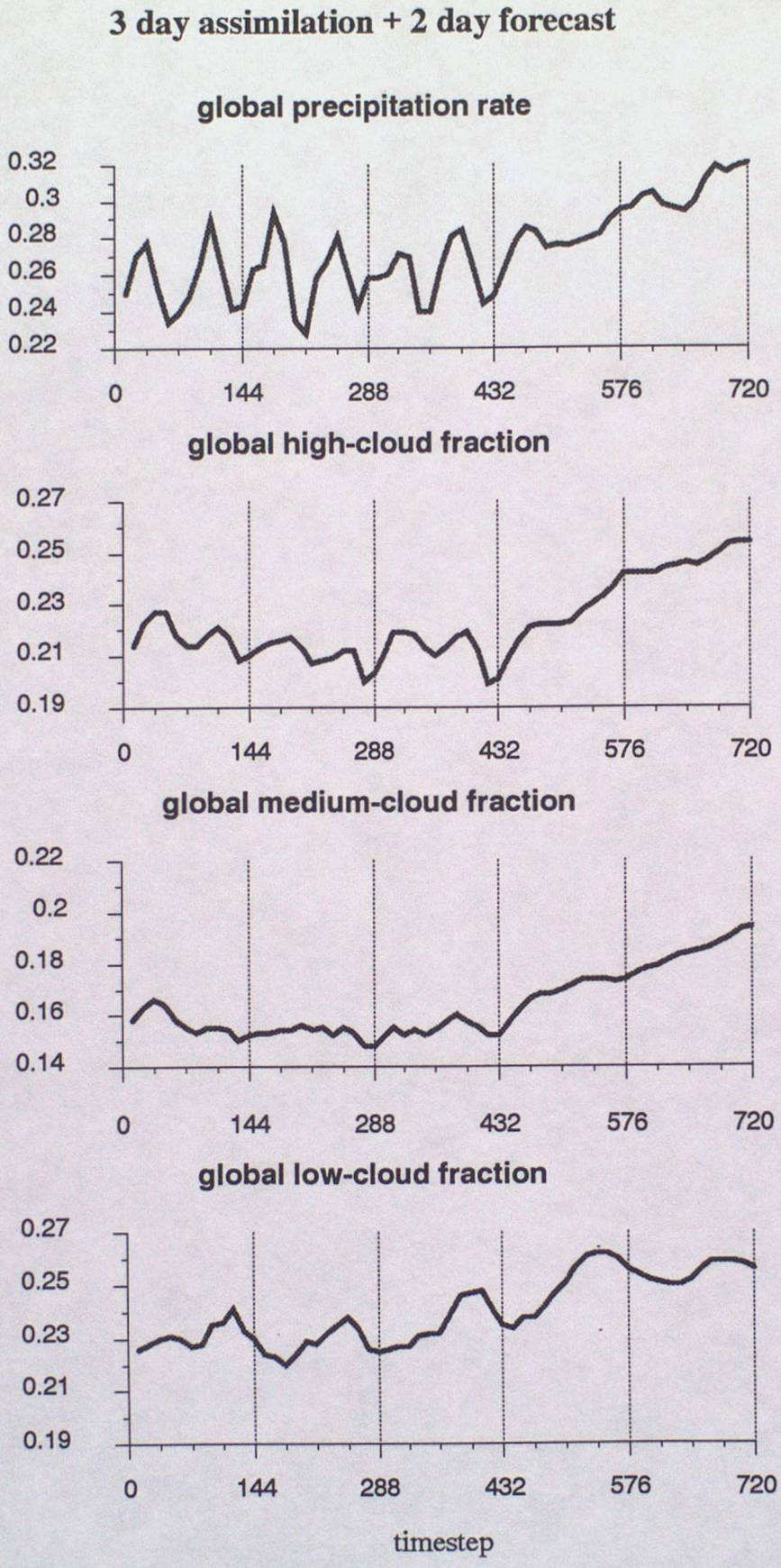

Figure 13 Time-series of global average precipitation rate (in 10^{-4} kg m^{-1} s^{-1}) and low medium and high fractional cloud cover, from the control experiment. This consisted of 3 days' assimilation (144 time-steps=1 day) followed by a 2 day forecast, for a case in October 1993.

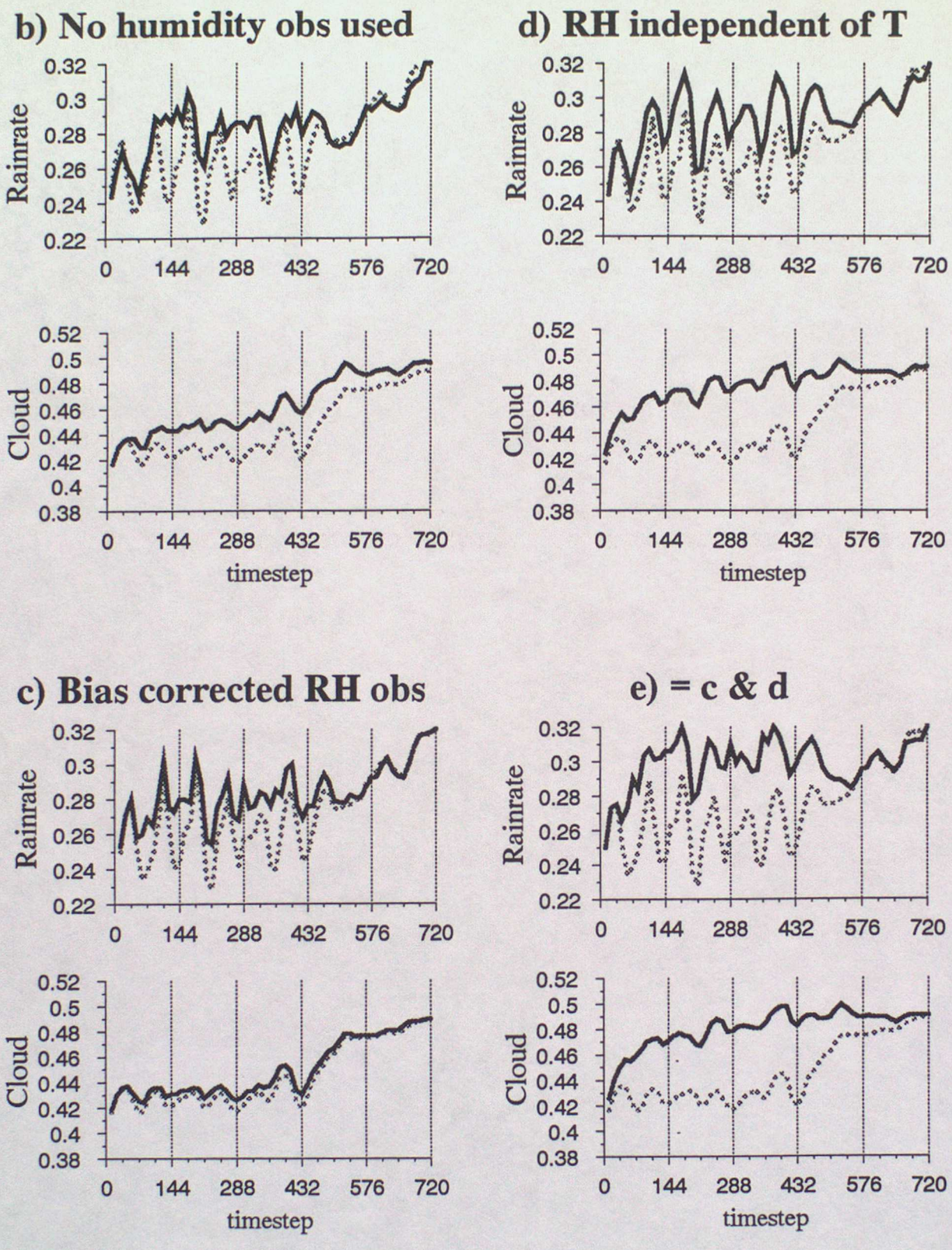

Figure 14 Time-series of global average precipitation rate (in 10^{-4} kg m^{-1} s^{-1}) and total fractional cloud cover, from the experiments listed in table 2, for a case in October 93. The plots each show one of experiments (b) (c) (d) or (e), with the control experiment (a) shown dotted.

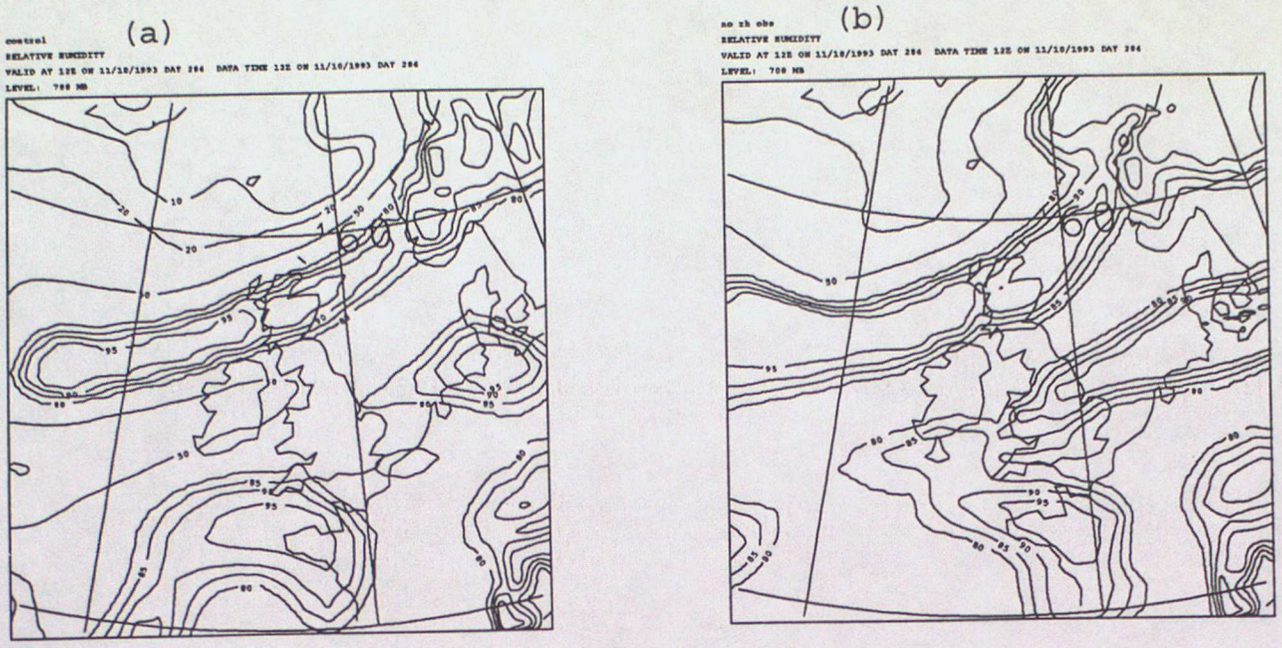

Figure 15 700hPa relative humidity field after 3 days' assimilation, for experiments (a) control, and (b) without humidity observations.

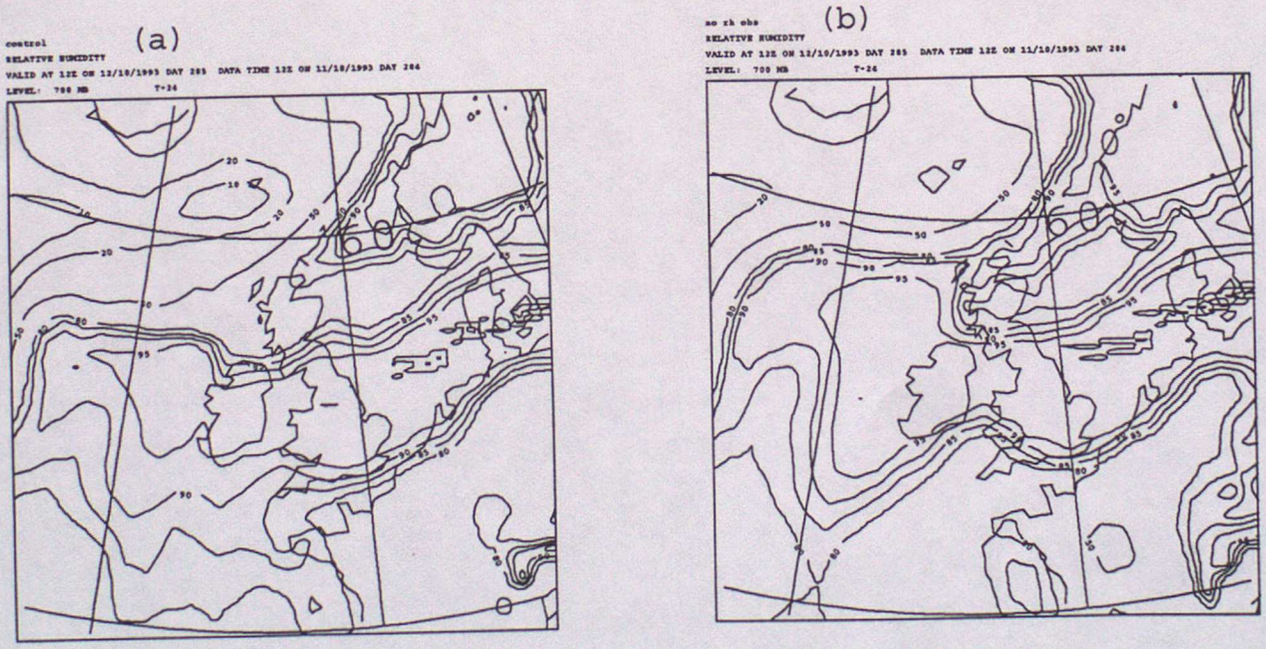

Figure 16 700hPa relative humidity field after 3 days' assimilation and 1 day forecast, for experiments (a) control, and (b) without rh observations.

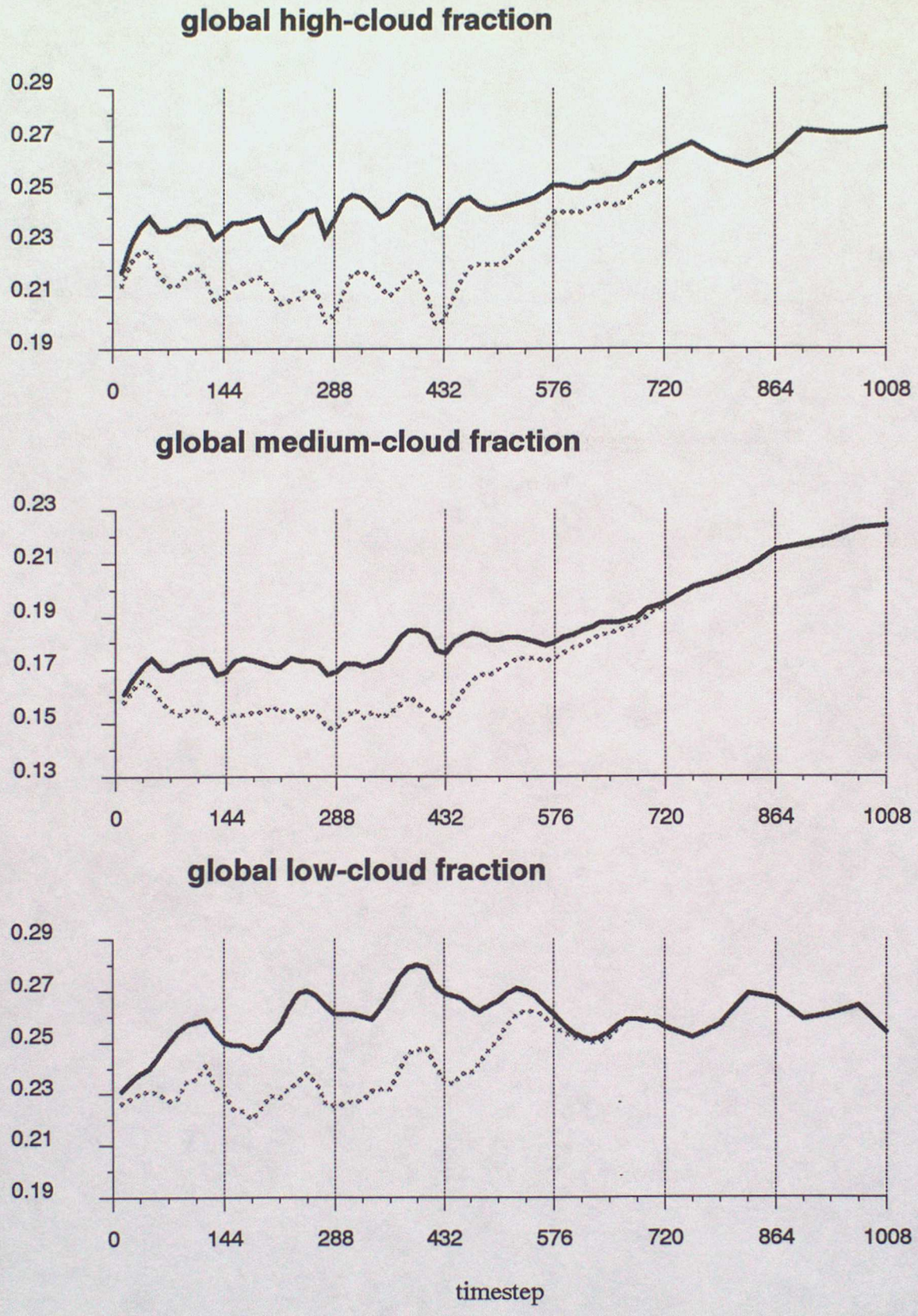

Figure 17 Time-series of low medium and high fractional cloud cover, from experiment (e). This consisted of 3 days' assimilation (144 time-steps=1 day) followed by a 4 day forecast. The control experiment (a), is shown dotted for comparison.